Traveling waves and localized modes in one-dimensional homogeneous granular chains with no precompression

Yuli Starosvetsky* and Alexander F. Vakakis†

Department of Mechanical Science and Engineering, University of Illinois at Urbana–Champaign, 1206 West Green Street, Urbana, Illinois 61822, USA

(Received 2 January 2010; published 20 August 2010)

We study a class of strongly nonlinear traveling waves and localized modes in one-dimensional homogeneous granular chains with no precompression. Until now the only traveling-wave solutions known for this class of systems were the single-hump solitary waves studied by Nesterenko in the continuum approximation limit. Instead, we directly study the discrete strongly nonlinear governing equations of motion of these media without resorting to continuum approximations or homogenization, which enables us to compute families of stable multihump traveling-wave solutions with arbitrary wavelengths. We develop systematic semianalytical approaches for computing different families of nonlinear traveling waves parametrized by spatial periodicity (wave number) and energy, and show that in a certain asymptotic limit, these wave families converge to the known single-hump solitary wave studied by Nesterenko. In addition, we demonstrate the existence of an additional class of stable strongly localized out-of-phase standing waves in perfectly homogeneous granular chains with no precompression or disorder. Until now such localized solutions were known to exist only in granular chains with strong precompression. Our findings indicate that homogeneous granular chains possess complex intrinsic nonlinear dynamics, including intrinsic nonlinear energy transfer and localization phenomena.

DOI: 10.1103/PhysRevE.82.026603 PACS number(s): 05.45.Yv, 45.70.−n

I. INTRODUCTION

Wave propagation in granular materials excited by various types of loads (single impacts, periodic or random sequences of impacts, harmonic forcings, etc.) is of significant practical importance in many applications. Indeed, it has been shown that granular media may serve as rather effective shock absorbers, e.g., granular layers from iron shot have been used for the dampening shocks in explosive chambers, and were shown to be effective mitigators of shock waves formed at the chamber walls. Granular materials constitute a class of highly nonlinear media where the commonly considered linear and weakly nonlinear approaches are far from being valid. This is due to the fact that contact forces in granular interfaces can be highly nonlinear, lacking linear terms. This led to the observation by Nesterenko [1] that an uncompressed homogeneous granular chain possesses zero speed of sound, leading to its characterization as *sonic vacuum*. Intuitively, one might conclude that due to complete lack of a linear structure in its dynamics such a medium could not support any form of coherent traveling waves. Yet, Nesterenko and co-workers [1–4] were the first to show that these media indeed can support a special solitary wave corresponding to no separation between beads. This work aims to extend this basic result by proving the existence of a whole class of stable traveling waves in these media, corresponding, however, to separations between beads and accumulating to the solitary wave studied by Nesterenko in a certain asymptotic sense.

The propagation of solitary waves in granular media in Hertzian contact is a subject of intense current study. The existence of a family of single-hump solitary waves in these media was first proved by Nesterenko and co-workers [2–4], whereas Coste *et al.* [5] reported a rather extensive experimental study of these waves. It is a well-known fact that these solitary waves propagate without distortion despite rather violent dispersion effects [1]. It is the balance of dispersion and nonlinearity that leads to spatially localized, coherent, and shape preserving propagating solitary waves with speed of propagation being directly proportional to the amplitude (energy). In two additional works general existence theorems for solitary waves in nonlinear [6] and granular [7] chains were proved, based on a general mathematical theorem restricted to one-dimensional nonlinear lattices given by Friesecke and Wattis [8].

The existence of spatially periodic traveling-wave solutions in one-dimensional granular chains of beads has been proven only for initially precompressed chains (see Nesterenko [1] for details), and to the best of the authors' knowledge existence of this type of waves in uncompressed granular media has not been reported before. Perhaps this is due to the fact that spatially periodic motions in granular media typically involve both separation and compression between adjacent beads, and therefore they cannot be resolved using analytical approaches based on continuous approximations or homogenization; this is due to the lack of analyticity of the interactive forces between beads. Instead, approaches that directly consider the discrete and strongly nonlinear equations of motion and can account for nonsmooth effects due to bead separation need to be followed.

A key to our work is the consideration of reduced-order granular chains with cyclicity or, equivalently, of finite granular chains with periodic boundary conditions. It is worthwhile noting that no damping is assumed in the contacts between the beads in our analysis. This idealization is

*staryuli@illinois.edu

†Corresponding author; avakakis@illinois.edu

necessary for studying the basic understanding of intrinsic dynamics of the spatially periodic waves in the considered granular media. In addition, conservation laws may also be formulated, leading to a substantial simplification of the dynamical analysis. In fact, gaining an understanding of the types of periodic waves of the purely elastic granular chains is a necessary initial step toward a future characterization of the traveling-wave dynamics of the corresponding weakly dissipative systems physical systems. Following our approach, nonlinear spatially periodic motions of the reduced-order cyclic systems correspond to spatially periodic traveling waves in granular chains of infinite spatial extent, with the periodicity (wave number) equal to the finite order of the reduced cyclic system. In this way, different families of strongly nonlinear periodic traveling-wave solutions can be studied systematically. Reduced-order systems with two-, three-, and four-bead cyclicities will be considered in detail, and the results will be extended to reduced systems with N-bead cyclicity. Following this approach we demonstrate the existence of a countable infinity of stable in-phase traveling waves with spatial periodicity. Along with these periodic traveling waves, a class of out-of-phase localized standing waves will also be demonstrated for the reduced system with three-bead cyclicity; we will conjecture that this family of localized standing waves exists for the systems with N-bead cyclicity.

The structure of the paper is as follows. Section II is devoted to the systematic description of the traveling-wave solutions for reduced systems with two-, three-, four-, and general N-bead cyclicities. In Sec. III we analyze in detail the single-hump solitary wave obtained in the limit $N\to\infty$ (first studied by Nesterenko), whereas convergence of the families of periodic traveling waves to the single-hump solitary wave in the limit of infinite cyclicity index $N\to\infty$ is performed in Sec. IV. We conclude in Sec. V with some closing remarks.

II. CYCLIC GRANULAR CHAINS WITH PERIODIC BOUNDARY CONDITIONS

Our study of nonlinear traveling and standing waves in homogeneous granular chains is based on the analysis of the dynamics of reduced-order homogeneous granular systems with periodic boundary conditions. Equivalently, these reduced systems may be regarded as finite-degree-of-freedom (DOF) granular systems with cyclicity (cyclic symmetry). By studying time-periodic orbits (or nonlinear normal modes (NNMs) [9–13]) of these reduced cyclic systems we can investigate the existence of traveling or standing waves with specific spatial periodicity (wave number) in homogeneous granular chains of infinite spatial extent. Our main interest lies in studying strongly nonlinear spatially periodic motions with constant but nontrivial phase shifts between adjacent beads, corresponding to traveling waves; the case of trivial (0 or π) phase shifts corresponds to standing waves which can be examined separately.

We start with the general definition of the reduced-order cyclic granular chain of N identical beads with periodic boundary conditions and no precompression, governed by

$$\ddot{u}_1 = (u_N - u_1)_+^{3/2} - (u_1 - u_2)_+^{3/2},$$

$$\ddot{u}_2 = (u_1 - u_2)_+^{3/2} - (u_2 - u_3)_+^{3/2},$$

$$\cdots$$

$$\ddot{u}_N = (u_{N-1} - u_N)_+^{3/2} - (u_N - u_1)_+^{3/2},$$

$$u_0 \equiv u_N, \quad u_{N+1} \equiv u_1, \tag{1a}$$

where $u_k(t)$ is the displacement of the kth bead, the (3/2) stiffness law models Hertzian contact between beads in compression, and the subscript (+) on the right-hand sides denotes that only positive arguments are allowed in the fractional powers, with the arguments being set equal to zero otherwise. This accounts explicitly for the possibility of *separation* between adjacent beads of the chain in the absence of compressive forces. Moreover, appropriate normalizations have been applied, so that all mass and stiffness coefficients are set equal to unity. System (1a) will be termed the *reduced granular system with* N-bead cyclicity. It should be clear that the dynamics of Eqs. (1a) can be directly extended to the corresponding granular chain of infinite spatial extent, since any solution of the N-bead reduced cyclic system represents also a spatially periodic solution of the infinite homogeneous granular chain which repeats itself every N beads (i.e., with N-bead cyclicity). Hence, we can extend the solutions of the N-bead cyclic system (1a) to the corresponding infinite chain through the relation $u_{p+mN}(t)=u_p(t)$ for $p=1,\ldots,N$, and $m=1,2,\ldots$

Focusing now on the strongly nonlinear system (1a), this admits two independent first integrals of motion corresponding to conservation of energy (E) and linear momentum (G) in the absence of external excitations:

$$E = \frac{\dot{u}_1^2}{2} + \frac{\dot{u}_2^2}{2} + \cdots + \frac{\dot{u}_N^2}{2} + \frac{2}{5}[(u_N - u_1)_+^{5/2} + (u_1 - u_2)_+^{5/2} + \cdots + (u_{N-1} - u_N)_+^{5/2}],$$

$$G = \dot{u}_1 + \dot{u}_2 + \cdots + \dot{u}_N = \text{const.} \tag{1b}$$

In addition to the above true first integrals of motion we will also impose the restriction that the initial velocity of center of mass of a cyclic chain is equal to zero, i.e., $G=0$. This restriction is necessary in order to study time-periodic motions in terms of bead displacements. The resulting additional restriction of zero initial velocity for the center of mass of the granular chain leads to the following constraint of motion which, however, is not a true first integral of motion:

$$C = u_1 + u_2 + \cdots + u_N = \text{const.} \tag{1c}$$

Without loss of generality this can be set equal to zero as the reference frame of the system can be arbitrary shifted; hence, from here on we will assume that $C=0$. Given that the reduced system possesses N DOF and there exist only two first integrals of motion, it is nonintegrable for $N>2$ and, hence, it is expected to possess complex dynamics (including chaotic orbits). The case $N=2$ is a special case since it corre-

sponds to a fully integrable, and hence, exactly solvable system.

As mentioned above, time-periodic solutions of Eqs. (1a) with nontrivial time delay (or, equivalently, phase difference) T between the displacements of adjacent beads correspond to traveling waves (with spatial periodicity equal to the cyclicity index N) in the corresponding infinite granular chain. These solutions are computed by reformulating Eqs. (1a) as a nonlinear delay differential equation (NDDE),

$$\ddot{u} = \{u(t-[N-1]T) - u(t)\}_+^{3/2} - [u(t) - u(t-T)]_+^{3/2},$$

$$u(t) = u(t+NT), \tag{2}$$

where T is the constant time shift between the motions of neighboring beads for a traveling-wave solution of Eqs. (1a). Clearly the NDDE (2) represents an infinite-dimensional dynamical system; however, as shown below its structure is suitable for deriving the amplitude-phase relations of the traveling-wave solutions and even for deriving analytical approximations in certain cases.

To initiate our study of Eq. (2) we introduce the rescalings

$$\tau = t/T, \quad \bar{u}(\tau) = T^4 u(\tau T), \tag{3}$$

which when substituted into Eq. (2) yield the following normalized NDDE:

$$\bar{u}'' = \{\bar{u}(\tau - 2[N-1]) - \bar{u}(\tau)\}_+^{3/2} - [\bar{u}(\tau) - \bar{u}(\tau-1)]_+^{3/2},$$

$$\bar{u}(\tau) = \bar{u}(\tau+N), \tag{4}$$

where primes denote differentiations with respect to the rescaled time τ. Clearly, time-periodic solutions of Eqs. (4) correspond to spatially periodic and time-periodic solutions of Eqs. (1a) corresponding to traveling waves. Assuming the existence of a time-periodic solution $\bar{\gamma}(\tau)$ of Eqs. (4) with constant amplitude $\bar{A}$, and using the rescalings (3), we obtain the following general relationship between the amplitude $\bar{A}$ and the nontrivial time shift T:

$$T^4 A = \bar{A} = \text{const}, \tag{5}$$

where A denotes the constant amplitude of the traveling wave in terms of the original (unscaled) coordinates. Relation (5) enables us to compute the amplitude-time shift relationship between all members of a particular family of traveling waves once a single member of that family has been computed. This important result will help us to develop important measures that will distinguish the different families of traveling waves in terms of their propagation speed. In particular, different families of traveling waves will be classified according to the cyclicity index N of the reduced system (4) (i.e., with respect to their wave numbers), whereas waves within the same family will be parametrized in terms of their amplitudes (or energies). In the following sections we will study in detail the families of traveling waves corresponding to cyclicity indices $N=2$, 3, and 4, and we will provide heuristic arguments regarding waves with general cyclicity index N.

Starting from the case $N=2$, the resulting fully integrable reduced system does not possess traveling-wave solutions,

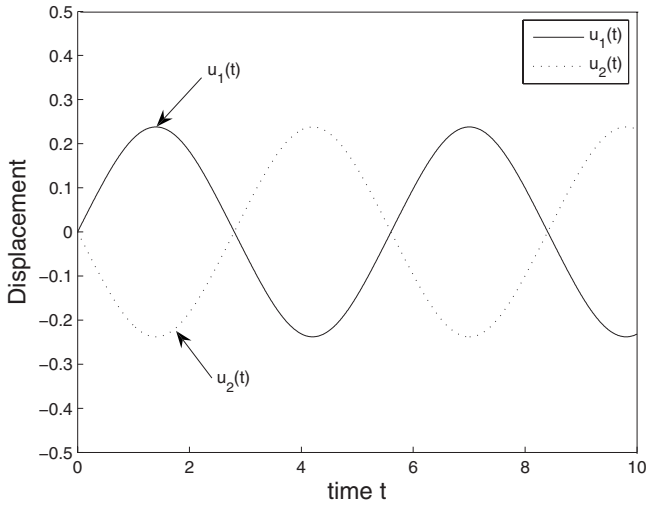

FIG. 1. Out-of-phase time-periodic standing wave corresponding to the reduced cyclic system with $N=2$.

but only out-of-phase standing waves (or NNMs [13]). As a result, the corresponding motion for the infinite granular chain is an out-of-phase time-periodic standing wave, with adjacent beads executing same amplitude but out-of-phase oscillations. Indeed, considering the governing equations for the two-bead reduced system,

$$\ddot{u}_1 = (u_2 - u_1)_+^{3/2} - (u_1 - u_2)_+^{3/2},$$

$$\ddot{u}_2 = (u_1 - u_2)_+^{3/2} - (u_2 - u_1)_+^{3/2}, \tag{6}$$

and imposing the constraint (1c) we obtain the single equation

$$\ddot{u}_1 = (-2u_1)_+^{3/2} - (2u_1)_+^{3/2}, \tag{7}$$

subject to initial conditions $u_1(0)=0$, $\dot{u}_1(0)=v$. This system can be solved explicitly,

$$t = {}_2F_1\left([2/5,1/2],[7/5],u^{5/2}\frac{b}{C}\right)\frac{1}{\sqrt{C}}u, \tag{8}$$

where ${}_2F_1(\cdot,\cdot,\cdot)$ is a hypergeometric function, $C=\beta u_{\max}^{5/2}$, and $\beta=2^{7/2}/5$. Expression (8) may be used to derive the relation between the amplitude of the standing wave and its period, by denoting the amplitude of the wave by $u_{\max}=A$, and computing the time shift as

$$T_P = 2T,$$

$$\frac{T_p}{4} = \frac{T}{2} = {}_2F_1\left([2/5,1/2],[7/5],A^{5/2}\frac{b}{C}\right)\frac{1}{\sqrt{C}}A, \tag{9}$$

where T_p is the period of the oscillation.

A typical member of this family of out-of-phase standing waves is depicted in Fig. 1. Considering the wave forms of the time series, they correspond to out-of-phase oscillations between adjacent beads, with complete absence of separation during the entire time-periodic oscillation. Hence, the case $N=2$ is nontypical, compared to the families of traveling waves corresponding to cyclicities $N>2$. Summarizing, the

reduced cyclic system with $N=2$ is fully integrable and can be resolved analytically. No conceptually new time-periodic motions are detected in that system since the computed family of out-of-phase NNM is quite intuitive due to the symmetry of the granular chain. As we will show below this does not hold for reduced systems with $N>2$, which possess complex and highly nontrivial time-periodic motions, including localized standing waves as well as traveling waves.

Examining first the case $N=3$, the governing equations of motion are given by

$$\ddot{u}_1 = (u_3 - u_1)_+^{3/2} - (u_1 - u_2)_+^{3/2},$$

$$\ddot{u}_2 = (u_1 - u_2)_+^{3/2} - (u_2 - u_3)_+^{3/2},$$

$$\ddot{u}_3 = (u_2 - u_3)_+^{3/2} - (u_3 - u_1)_+^{3/2}. \tag{10}$$

The dynamics of system (10) is too complicated to be amenable to straightforward analytical treatment since it represents a three-DOF strongly nonlinear nonsmooth dynamical system with only two first integrals of motion, so it is nonintegrable. However, as discussed below, it is still possible to perform a full study of the time-periodic orbits of Eqs. (10) by constructing Poincaré maps at fixed energy levels.

To this end we resort to the two first integrals of motion (1b) and the imposed constraint (1c). Applying first Eq. (1c) to system (10) this can be further reduced to the following two-DOF system:

$$\ddot{u}_1 = (-u_2 - 2u_1)_+^{3/2} - (u_1 - u_2)_+^{3/2},$$

$$\ddot{u}_2 = (u_1 - u_2)_+^{3/2} - (2u_2 + u_1)_+^{3/2}, \tag{11}$$

which possesses the additional first integral E denoting conservation of total energy:

$$E = \frac{(\dot{u}_1)^2}{2} + \frac{(\dot{u}_2)^2}{2} + \frac{(\dot{u}_1 + \dot{u}_2)^2}{2} + \frac{2}{5}[(-u_2 - 2u_1)_+^{5/2} + (u_1 - u_2)_+^{5/2} + (2u_2 + u_1)_+^{5/2}]. \tag{12}$$

Hence, it is possible to fully study the global dynamics of Eqs. (11) by constructing two-dimensional Poincaré maps [14]. To this end, we fix the total energy E to a constant level, thus restricting the dynamical flow of Eqs. (11) to a three-dimensional isoenergetic manifold. This is performed by imposing the following condition (which also holds at $t=0$):

$$E(u_1, \dot{u}_1, u_2, \dot{u}_2) = h, \tag{13}$$

where h is a constant. By transversely intersecting [14] the three-dimensional isoenergetic manifold (13) by the two-dimensional cut plane $T:\{u_1=0\}$, we construct the two-dimensional Poincaré map $P:\Sigma \to \Sigma$, where the Poincaré section Σ is defined as

$$\Sigma = \{u_1 = 0,\ \dot{u}_1 > 0\} \cap \{E(u_1, \dot{u}_1, u_2, \dot{u}_2) = h\}. \tag{14a}$$

It is worthwhile mentioning that the Poincaré section could also be defined in the original three-DOF system (10) as follows:

$$\Sigma = \{u_1 = 0,\ \dot{u}_1 > 0\} \cap \{G(\dot{u}_1, \dot{u}_2, \dot{u}_3) = 0\} \cap \{E(u_1, \dot{u}_1, u_2, \dot{u}_2, u_3, \dot{u}_3) = h\}, \tag{14b}$$

where the restriction $\dot{u}_1 > 0$ is imposed so that the Poincaré map is orientation preserving.

Fundamental time-periodic solutions of basic period T_p of Eqs. (10) correspond to period-1 equilibrium points of the Poincaré map, i.e., to orbits of the dynamical system that recurrently pierce the cut section Σ at a single point. Additional *subharmonic* solutions of periods nT_p may exist corresponding to period-n equilibrium points of the Poincaré map, i.e., to orbits that pierce the cut section n times before repeating themselves. Moreover, the stability properties of these stationary orbits can be fully explored by studying the topologies of nearby orbits in the Poincaré map. Hence, if an equilibrium point of the Poincaré map [i.e., a time-periodic orbit of system (10)] appears as a center, i.e., surrounded by closed curves resulting from intersections of invariant tori of the dynamics with the cut plane Σ, then the solution is orbitally stable. If, on the contrary, an equilibrium of the Poincaré map appears as a saddle point, then the corresponding time-periodic solution of Eqs. (10) is orbitally unstable and, hence, not physically realizable.

Before proceeding to the discussion of the results, a note on the use of Poincaré maps for studying strongly nonlinear dynamics of coupled oscillators is appropriate. Indeed, Poincaré maps are highly significant in studying the global dynamics of nonlinear systems with low dimensionality (such as the reduced cyclic system with $N=3$) since they provide us with full description of all types of regular and chaotic motions that can be realized. In fact, one of the well-known applications of Poincaré maps is for the weakly perturbed integrable systems where according to the Kolmogorov-Arnold-Mmoser theorem [14] the breakup of "rational tori" and preservation of "sufficiently irrational tori" may be observed in the map (the interested reader is referred to [14]). It is important to emphasize that the system under investigation [Eqs. (10)] is far from being integrable (and it cannot be characterized as near integrable either), so in addition to "regular" type of dynamics (e.g., standing and traveling waves) it possesses "nonregular" dynamics in the form of chaotic orbits exhibiting sensitive dependence on initial conditions. This can be clearly deduced from the results below where a "stochastic sea" of chaotic orbits is shown to encircle "islands" of regular dynamics. Despite the complexity of the dynamics of system (10), the Poincaré maps are rather useful for systematically finding *all* types of time-periodic regular orbits that coexist with chaotic ones in this highly degenerate, nonsmooth, and strongly nonlinear system. In addition, Poincaré maps also provide us with information regarding the stability and robustness of these time-periodic regimes, which is important in proving physical realization of the computed time-periodic orbits.

The Poincaré map P of system (10) is illustrated in Fig. 2 for the fixed energy level $h=0.1$. We note that the dynamics is complex, with large regions of the phase space filled by chaotic orbits. In addition, numerous stable fundamental and subharmonic time-periodic orbits are detected, including the fundamental periodic orbits A–D and the subharmonic orbit

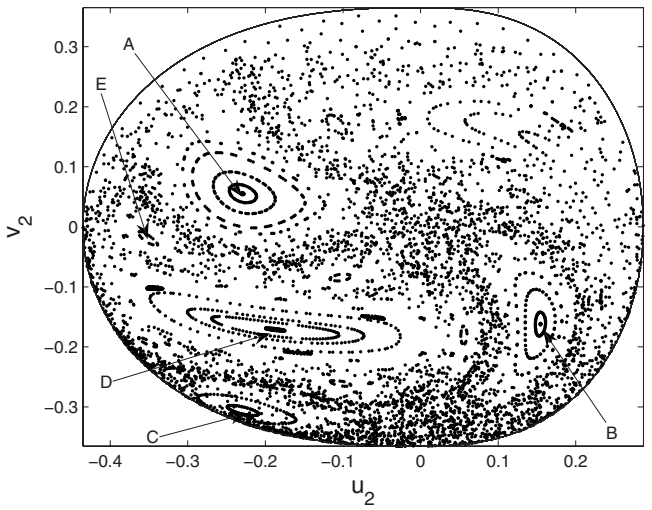

FIG. 2. Two-dimensional Poincaré maps of system (10) at fixed energy levels; $h=0.1$.

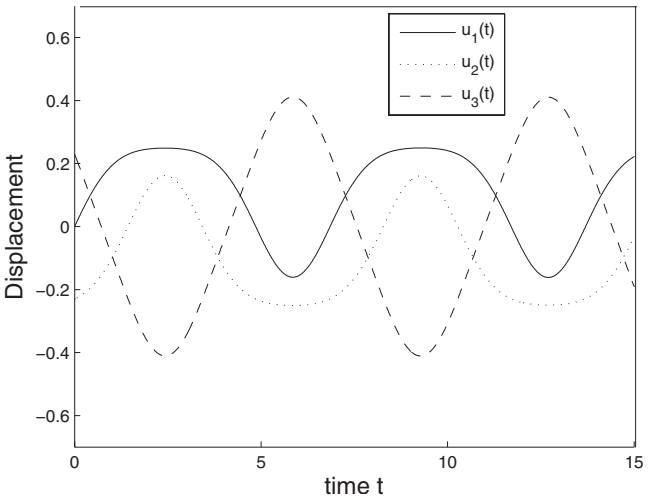

FIG. 4. Localized NNM for $N=3$ and energy level $h=0.1$ (point A in Fig. 2).

E. Additional stable subharmonic orbits exist in this system with smaller domains of attraction and hence not easily detectable in the Poincaré map. A typical subharmonic orbit corresponding to the equilibrium points E of the Poincaré map in Fig. 2 is presented in Fig. 3; in this orbit the central bead (bead 2) oscillates two times faster than its neighbors. We conjecture that a countable infinity of these subharmonic orbits exist in this system, as this is typical in nonintegrable dynamical systems [14].

Two main types of stable fundamental orbits are detected in the Poincaré maps. The first type corresponds to the stable period-1 equilibrium points A–C in Fig. 2, and are localized standing waves (NNMs) where all beads execute synchronous oscillations with energy being predominantly localized to a single bead. The localized NNM corresponding to equilibrium point A of the Poincaré map in Fig. 2 is depicted in Fig. 4. We note that the amplitude of oscillation of bead 3 of the reduced system is larger than the amplitudes of the other two beads, which oscillate in an out-of-phase fashion with respect to it. Due to the cyclic symmetry of Eqs. (10) two additional localized NNMs exist corresponding to the equilibrium points B and C of the Poincaré map in Fig. 2, with the wave forms of oscillations of the beads (and of localization) being cyclically interchanged. This is a rather obvious consequence from the viewpoint of the cyclic symmetry of the reduced three-bead system. Clearly, these results can be extended to the infinite granular chain by repeating the wave forms in Fig. 4 every three beads; this proves the existence of a standing wave in the homogeneous granular chain with recurring localization every three beads.

The second type of fundamental time-periodic orbits corresponds to the stable period-1 equilibrium point D of the Poincaré map, and is depicted in Fig. 5. Clearly it corresponds to the previously discussed traveling-wave solution (i.e., a time-periodic solution with a constant but nontrivial shift in phase between adjacent beads). The period of this traveling wave is equal to exactly three times the time shift T, $T_p=3T$. Hence, the three-bead reduced cyclic system is the

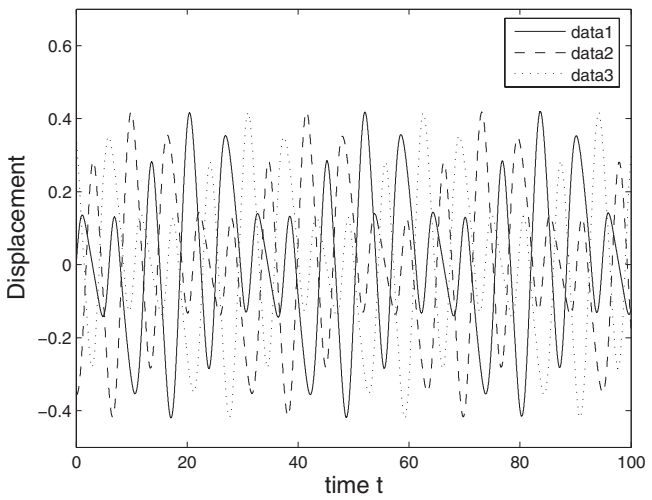

FIG. 3. Subharmonic orbit for $N=3$ and energy level $h=0.1$ (point E in Fig. 2).

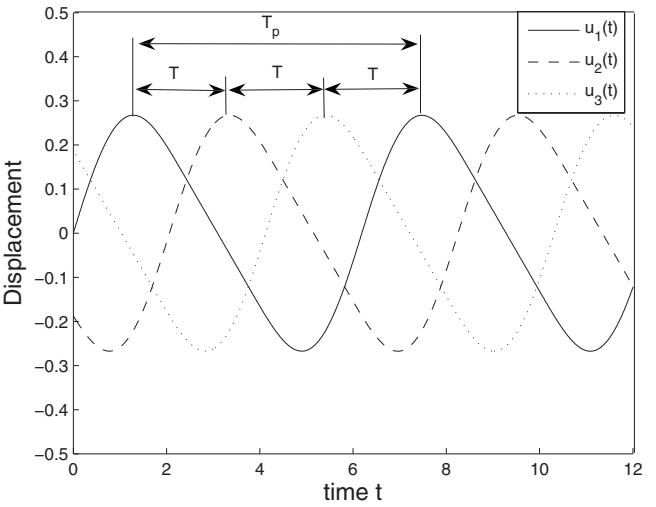

FIG. 5. Traveling-wave solution for $N=3$ and energy level $h=0.1$ (point D in Fig. 2).

lowest order of such system that admits a family of traveling waves. Members of this family are parametrized by energy (i.e., the wave amplitude). Considering the wave form of the traveling wave, we note its clear *asymmetry*. This is a consequence of the fact that during traveling-wave propagation there exist two distinct regimes in the motion of each bead; a regime of "smooth dynamics" during which each bead is in contact and interacts through Hertzian compressive forces with its neighbors and a regime of "nonsmooth dynamics" where separation between beads takes place, and the bead is in "free flight" before colliding with its neighbor. These two regimes continuously interchange during the propagation of the traveling wave through the homogeneous granular chain and give rise to multiphase strongly nonlinear dynamical effects. We note that by adding precompression (in this study it is assumed to be zero) the regime of free flight is significantly affected or even completely eliminated, so the dynamics change quantitatively, becoming weakly nonlinear [15,16]. In the absence of precompression, however, the strongly nonlinear and nonsmooth nature of the dynamics should be taken explicitly into account when studying the different families of traveling waves considered herein.

Before proceeding to higher-DOF reduced cyclic systems and examining additional families of traveling waves, we note that the period T_p (and the time shift T) depends nonlinearly on the amplitude of the wave oscillation [see relation (5)]. It follows that there exists a continuous family of spatially periodic traveling waves with three-bead periodicity, parametrized by the wave amplitude.

Increasing the cyclic periodicity index to $N=4$, we consider the following governing equations of motion:

$$\ddot{u}_1 = (u_4 - u_1)_+^{3/2} - (u_1 - u_2)_+^{3/2},$$

$$\ddot{u}_2 = (u_1 - u_2)_+^{3/2} - (u_2 - u_3)_+^{3/2},$$

$$\ddot{u}_3 = (u_2 - u_3)_+^{3/2} - (u_3 - u_4)_+^{3/2},$$

$$\ddot{u}_4 = (u_3 - u_4)_+^{3/2} - (u_4 - u_1)_+^{3/2}. \quad (15)$$

This dynamical system is again nonintegrable and of higher dimensionality, so it is not amenable to analytical or numerical study based on Poincaré map constructions. Hence, we focus exclusively on the direct numerical computation of the family of traveling waves. The wave form of the traveling wave for the system with four-bead periodicity is depicted in Fig. 6, from which its asymmetric nature is evident. As discussed previously this asymmetry is a consequence of nonsmooth dynamics caused by separation between beads. Unlike the previously considered reduced systems there is no systematic approach for analyzing the dynamics for $N=4$ cyclicity, but using the first integrals of motion (1b) the dimensionality may be reduced. The period of this wave family is exactly equal to four times the time shift, $T_p=4T$, and the general relation (5) can be used to find the characteristic amplitude-time shift (or amplitude-speed) relationship for this family of traveling waves. Given the complexity of the problem, the particular solution for the four-bead cyclic chain was computed numerically in an *ad hoc* fashion, i.e., by adopting a numerical optimization scheme.

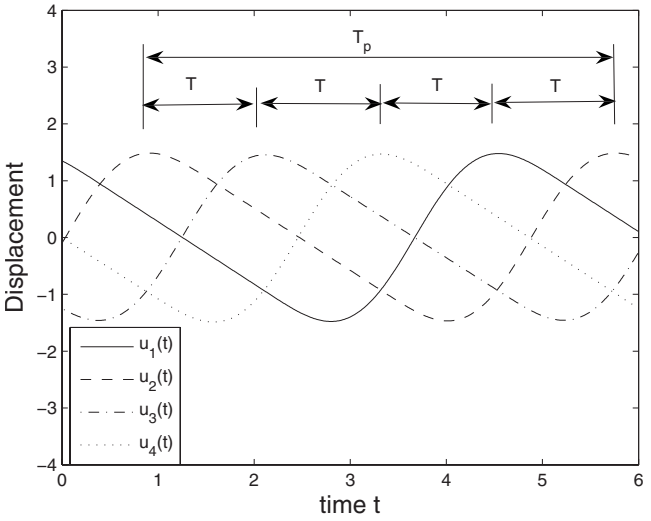

FIG. 6. Traveling-wave solution for $N=4$ and energy level $h=0.1$.

Comparing the wave forms of the traveling waves for $N=3$ (Fig. 5) and $N=4$ (Fig. 6) we conclude that *the asymmetry increases with increasing cyclic periodicity index N*. This is a direct consequence of the fact that with increasing periodicity index the regime of free flight (or bead separation) is of longer duration compared to the regime of beads in compression. This raises the obvious question related to the asymptotic limit of the wave form of the traveling wave as we take $N \to \infty$. Although a full analytical description of this asymptotic process is still lacking, the following formulation provides heuristic arguments and hints toward answering this question.

Let us start with an important observation. As the nonlinear interaction potential between beads becomes stiffer, i.e., the (3/2) power-law Hertzian interaction is replaced with a general $(n/2)$ power law with $n \to \infty$, the dynamical response of the system tends to the limiting case of *vibroimpact response*. This type of response was studied extensively by Pilipchuk and co-workers [17–21] by means of a special class of nonsmooth coordinate transformations based on sawtooth function. In Pilipchuk's works these sawtooth functions were successfully used as generating solutions for strongly nonlinear perturbation schemes together with special algebras that were specially developed for analytically studying strongly nonlinear dynamics close to vibroimpact ones (see Pilipchuk [17–19] for details). For the specific problem of traveling-wave computation in the granular chain with N-bead cyclicity the following normalized nonsmooth functions are introduced:

$$\tau(t,\gamma) = \begin{cases} t/(1-\gamma), & -1+\gamma \le t \le 1-\gamma \\ (-t+2)/(1+\gamma), & 1-\gamma \le t \le 3+\gamma, \end{cases}$$

$$e(t,\gamma) = \frac{\partial \tau(t,\gamma)}{\partial t},$$

$$\tau(t,\gamma) = \tau(t+4,\gamma), \quad 0 \le \gamma < 1. \tag{16}$$

As one may note from Eqs. (16) the sawtooth functions possess asymmetry governed by the parameter γ. This type of asymmetric nonsmooth transformation has also been studied by Pilipchuk and co-workers [20,21]. Considering first the vibroimpact limit, that is, the case of perfectly elastic vibroimpact interactions between neighboring beads, traveling waves can be conveniently expressed in terms of the nonsmooth functions (16) as

$$u_0(t) = A\tau(t/a,\gamma),$$

$$u_i(t) = A\tau([t-iT]/a,\gamma), \quad i = \pm 1, \pm 2, \ldots,$$

$$a = T_p/4 = NT/4, \tag{17}$$

where a is the quarter period of the periodic response, N is the index of cyclicity, and $0 \le \gamma < 1$ is a coefficient governing the asymmetry in the wave form; for $\gamma=0$ the wave form is perfectly symmetric, whereas in the limit $\gamma \to 1$ the wave form becomes completely asymmetric and the temporal and spatial periodicities are lost. The heuristic form (17) is justified by the argument that for a traveling wave in the chain with vibroimpacts (i.e., in the limit $n \to \infty$) each bead undergoes a periodic series of perfectly elastic vibroimpacts (pulses of infinitely small duration) when it collides with its neighbors, whereas in between impacts it performs free flight with constant velocity. Moreover, bearing in mind the constraint formulated in Eq. (1c) (i.e., that the granular chain has a stationary center of mass) we deduce the following relation:

$$G = \sum_{i}^{N} \dot{u}_i = 0. \tag{18}$$

Then, according to Eqs. (16) and (17) each bead during its free flight regime can have only two possible velocities which are easily computed as

$$\dot{u}_i(t) = \pm A/(1 \mp \gamma) \quad \text{(regimes of free flight)}. \tag{19a}$$

One of the possible ways for the beads of the vibroimpact chain to satisfy both relations (18) and (19a) during free flight is that at any instant of time the velocity of only one of the beads is positive with the rest having identical but negative velocities; this would lead to the following relation which determines the coefficient of asymmetry for traveling-wave propagation in the vibroimpact N-DOF cyclic chain:

$$1/(1-\gamma) = (N-1)/(1+\gamma) \Rightarrow \gamma = (N-2)/N. \tag{19b}$$

Moreover, due to the assumption of perfectly elastic impacts, at each collision the impacting beads will completely interchange their velocities and will perform identical but time-shifted periodic motions. We note that although our previous assumption concerning the bead velocities is not the only possible one for chains with cyclicity index $N>2$, however, our numerical simulations confirm this conjecture.

From Eq. (19b) it follows that for two-bead cyclicity it holds that $\gamma=0$; for three-bead cyclicity we get $\gamma=1/3$; for four-bead cyclicity $\gamma=1/2$; and, finally, for $N \to \infty$ the asymmetry coefficient reaches the asymptotic limit $\gamma \to 1$. It is clear from a geometric viewpoint that $\gamma=0$ corresponds to a symmetric wave form as expected for the out-of-phase standing wave of the system with two-bead cyclicity, whereas the other limit $\gamma \to 1$ corresponds to complete asymmetry that eliminates the temporal and spatial periodicities of the wave form of the traveling wave and leads to an infinite period of oscillation. In fact, the perfectly asymmetric limit $N \to \infty$ corresponds to a single-hump solitary wave which is the vibroimpact analog of the solitary wave studied by Nesterenko and Lazaridi [2,4] and Chatterjee [3] in homogeneous granular chains.

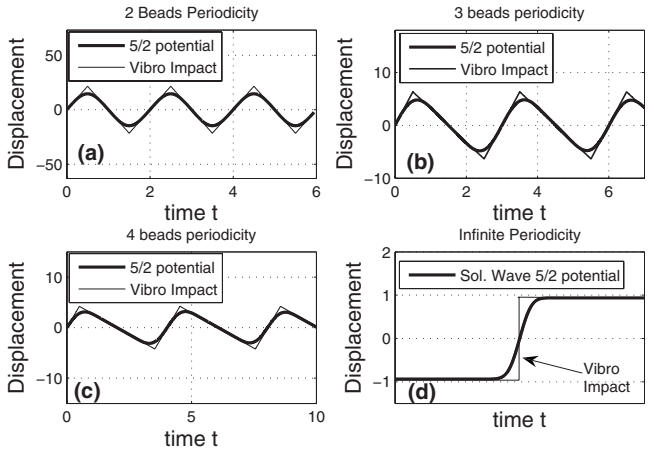

FIG. 7. Comparison of wave forms of traveling waves for chains with vibroimpact ($n \to \infty$) and Hertzian ($n=5/2$) potentials: (a) $N=2$, (b) $N=3$, (c) $N=4$, and (d) $N \to \infty$ (solitary wave studied by Nesterenko).

When Hertzian law interaction potential is considered instead of vibroimpact potential, the corresponding traveling waves are close to the vibroimpacting traveling waves as can be deduced from the plots in Fig. 7. These results demonstrate the close relation between vibroimpact traveling waves in chains of particles with infinitely stiff interaction potentials and strongly nonlinear traveling waves in granular chains with Hertzian interaction potentials. Based on this observation analytical approximations can be constructed for studying the different families of traveling waves in the homogeneous granular chain using the nonsmooth (sawtooth) solutions as generating functions [17–19]. The resulting analytical approximations will be valid for strongly nonlinear dynamical regimes, in contrast to traditional perturbation techniques based on linearized (harmonic) generating solutions which are only valid in weakly nonlinear regimes.

In what follows we provide an outline of this analysis. We will seek time- (and spatially) periodic solutions of Eqs. (1a) by expressing them in terms of the two sawtooth functions (16). As a result, we reduce the problem to a two-point nonlinear boundary value problem (NBVP) in the finite interval $-1 \le \tau \le +1$; by construction, the solutions of the NBVP would then correspond to time-periodic solutions of the original system (1a). To this end, we express the dynamical system (1a) with cyclicity index N in the following vector form:

$$\ddot{\underline{u}}(t) = f(\underline{u}(t)), \quad f:R^N \to R^N,$$

$$f(\underline{u}(t)) = \begin{pmatrix} (u_N - u_1)_+^{3/2} - (u_1 - u_2)_+^{3/2} \\ (u_1 - u_2)_+^{3/2} - (u_2 - u_3)_+^{3/2} \\ \cdots \\ (u_{N-1} - u_N)_+^{3/2} - (u_N - u_1)_+^{3/2} \end{pmatrix}, \tag{20a}$$

where $\underline{u}(t)=[u_1(t),u_2(t),u_3(t),\ldots,u_N(t)]^T$ is the N vector of bead displacements and from here on underline denotes an N vector. As demonstrated by Pilipchuk [17–19] any time-periodic solution of the dynamical system (20a) [or, equivalently, of system (1a)] may be expressed in the following form:

$$\underline{u}(t) = \underline{X}(\tau(t)) + e(t)\underline{Y}(\tau(t)), \tag{20b}$$

where $\tau=\tau(t,\gamma)$, $e=e(t,\gamma)$ are the sawtooth functions (16), and the displacement of the ith bead is expressed in terms of the sawtooth functions as $u_i=X_i(\tau)+Y_i(\tau)e$, with $i=1,\ldots,N$. Then, we assemble the components of the expansions of the displacements in the N vectors $\underline{X}=[X_1,X_2,X_3,\ldots,X_n]^T$ and $\underline{Y}=[Y_1,Y_2,Y_3,\ldots,Y_n]^T$. Before proceeding with the formulation of the NBVP in terms of the vectors $\underline{X}$ and $\underline{Y}$, we comment on an important multiplication property of the algebra defined by expansion (20b),

$$e(\tau,\gamma)\cdot e(\tau,\gamma) = \alpha + \beta e(\tau,\gamma), \tag{20c}$$

where $\alpha=1/(1-\gamma^2)$ and $\beta=2\gamma\alpha$, and from here on we omit the explicit dependence of the variables on t. This relation enables us to express the product (20c) in terms of the algebra defined by Eq. (20b). Differentiating Eq. (20b) once with respect to time we obtain,

$$\dot{\underline{u}} = \underline{X}'e + \underline{Y}'e^2 + \underline{Y}\frac{de}{dt} = \underline{X}'e + \underline{Y}'(\alpha+\beta e) + \underline{Y}\frac{de}{dt}, \tag{20d}$$

where prime denotes differentiation with respect to τ, and overdot with respect to time t. Note that the last term of Eq. (20d) contains singularities of first kind at the set of points $\Lambda=\{t\in R/\tau(t)=\pm 1\}$. Since $\dot{\underline{u}}(t)$ should be a continuous function of t it is necessary to eliminate these singularities by imposing the requirement

$$\underline{Y}|_{\tau=\pm 1} = 0, \tag{20e}$$

which provides one set of boundary conditions for the NBVP. An additional set of boundary conditions is obtained by differentiating (20d) once more leading to the expression

$$\ddot{\underline{u}} = \alpha\beta\underline{Y}'' + \alpha\underline{X}'' + e[(\beta^2+\alpha)\underline{Y}'' + \beta\underline{X}''] + (\beta\underline{Y}' + \underline{X}')\frac{de}{dt}. \tag{20f}$$

Similar arguments regarding smoothness of $\ddot{\underline{u}}(t)$ lead to the additional requirement

$$(\beta\underline{Y}' + \underline{X}')|_{\tau=\pm 1} = 0. \tag{20g}$$

Returning to Eqs. (20a), its right-hand side may also be expressed in terms of the algebra (20b) as follows [17–19]:

$$f(\underline{u}) = \underline{R}_f(\tau) + e\underline{I}_f(\tau),$$

$$\underline{R}_f(\tau) = (1/2\alpha)\left[\frac{1}{1+\gamma}f(\underline{Z}_+(\tau)) + \frac{1}{1-\gamma}f(\underline{Z}_-(\tau))\right],$$

$$\underline{I}_f(\tau) = (1/2\alpha)[f(\underline{Z}_+(\tau)) - f(\underline{Z}_-(\tau))], \quad \underline{Z}_\pm(\tau) = \underline{X}(\tau) \pm \frac{\underline{Y}(\tau)}{1\mp\gamma}. \tag{20h}$$

Substituting Eqs. (20f) and (20h) in Eqs. (20a), and taking into account the smoothness conditions (20e) and (20g) we obtain the following transformed dynamical system in terms of the considered algebra:

$$\alpha\beta\underline{Y}''(\tau) + \alpha\underline{X}''(\tau) + e[(\beta^2+\alpha)\underline{Y}''(\tau) + \beta\underline{X}''(\tau)] = \underline{R}_f(\tau) + e\underline{I}_f(\tau),$$

$$\underline{Y}|_{\tau=\pm 1} = 0, \quad (\beta\underline{Y}' + \underline{X}')|_{\tau=\pm 1} = 0. \tag{20i}$$

Setting separately [17–19] the components of Eqs. (20i) depending or not on e, following writing of Eqs. (20a) in terms of sawtooth functions, yields the following two-point NBVP in the interval $-1\le\tau\le+1$:

$$\alpha^2\underline{Y}''(\tau) = \alpha\underline{I}_f(\tau) - \beta\underline{R}_f(\tau),$$

$$\alpha^2\underline{X}''(\tau) = (\beta^2+\alpha)\underline{R}_f(\tau) - \alpha\beta\underline{I}_f(\tau),$$

$$\underline{Y}'|_{\tau=\pm 1} = 0, \quad (\beta\underline{Y}' + \underline{X}')|_{\tau=\pm 1} = 0. \tag{20j}$$

It is important to note that the NBVP (20j) is rather complicated, and even its numerical solution poses distinct challenges. Interestingly enough, analytical approximations may be developed for this problem by the following the method of successive approximations in the interval $-1\le\tau\le+1$ as outlined by Pilipchuk [17–19]. In that regard the choice of generating solutions for these successive approximations is crucial. To this end, the wave forms of the previously discussed traveling waves in vibroimpacting particle chains can offer excellent candidates for generating solutions; this should be clear when comparing the wave forms of the traveling waves in the granular chain to those of the vibroimpacting waves depicted in Fig. 7. Deriving analytical approximations to the NBVP is beyond the scope of the present paper which is left as an open problem.

In summary, our results indicate that in the homogeneous granular chain of infinite spatial extent there exists a countable infinity of families of stable traveling waves. Different families of waves are parametrized by the index of cyclicity $N>2$, whereas waves within the same family are parametrized by energy (i.e., their amplitude). The speeds of propagation of the traveling waves strongly depend on their amplitude as they are strongly nonlinear; however, they are smaller than the corresponding speed of propagation of the single-hump solitary wave studied by Nesterenko. The nonlinearity of the wave motion is caused not only by the fractional power of the Hertzian interaction between beads, but also by nonsmoothness effects due to bead separation and collision in regimes of free flight. These strong nonlinearities

pose distinct challenges when trying to analytically study these waves, but our approach based on direct analysis of the discrete equations of motion and on cyclic periodicity can provide some useful hints regarding their properties. Clearly, the nonsmooth character of this class of traveling waves prevents the application of techniques based on continuum approximations for their study.

Since the solitary wave obtained in the limit $N\to\infty$ can be considered as an asymptotic limit of this countable infinity of families of traveling waves (see previous discussion), in the next section we focus exclusively on this wave and provide an analytical approach based on Padé approximations to accurately analyze its wave form.

III. ANALYSIS OF THE SOLITARY WAVE IN THE LIMIT $N\to\infty$

In the limit $N\to\infty$ we can analytically approximate the solitary traveling wave using Padé approximants. Our analysis provides accurate approximations of the wave form, with the accuracy improving as the number of terms included in the Padé approximations increases. Moreover, our analysis provides a direct analytical estimate of the dependence of the speed of the wave on its amplitude. A similar analysis has been reported by Sen *et al.* [22] based on the use of exponential Padé approximants and numerical estimations of wave speed from numerical experiments. The importance of accurately computing the single-hump solitary wave in the limit $N\to\infty$ derives from the fact that this wave is typically formed in granular chains excited by impulse excitation in one of their beads. Numerical, experimental, and analytical studies have shown that, typically [1,22–24], as the pulse propagates through the granular chain this solitary wave develops in space and time. It follows that this solitary wave is a fundamental dynamical mechanism for energy transfer through homogeneous granular media.

Considering the reduced system (1a) in the limit $N\to\infty$,

$$\ddot{u}_n = (u_{n-1}-u_n)_+^{3/2} - (u_n - u_{n+1})_+^{3/2}, \quad -N \le n \le N, \quad N\to\infty, \tag{21}$$

we seek a traveling-wave solution whose wave form remains unchanged as it propagates through the granular chain. As shown previously [see relation (2)], by introducing the notion of time delay T between the displacements of adjacent beads, it is possible to reformulate this problem in terms of a nonlinear delay differential equation (NDDE). It will be helpful at this point if we use as coordinates the relative displacements δ_n between adjacent beads,

$$\delta_n = (u_n - u_{n+1}), \tag{22}$$

and transform Eq. (21) in the form

$$\ddot{\delta}_n = (\delta_{n-1})_+^{3/2} - 2(\delta_n)_+^{3/2} + (\delta_{n+1})_+^{3/2},$$

$$-N \le n \le N, \quad N\to\infty. \tag{23}$$

Then, using the arguments that led to the NDDE (2), we formulate the following NDDE describing the sought traveling-wave solution:

$$\ddot{\delta} = [\delta(t-T)]_+^{3/2} - 2(\delta)_+^{3/2} + [\delta(t+T)]_+^{3/2},$$

$$\delta(t) = \delta(t+NT), \quad N\to\infty, \tag{24}$$

where following the notation of the previous section, T is the constant (phase) time shift of the traveling wave between any adjacent beads. Following the solitary solution developed by Nesterenko [1], we will develop a Padé approximation of the solution of Eqs. (24) in the form of a localized motion that decays at infinity. Indeed, assuming a localized solitary structure for the solution (single hump) we introduce the restrictions

$$\delta(0) \ge \delta(t), \quad \delta(t\to\pm\infty) = 0. \tag{25}$$

Performing another change of variables,

$$\delta_n = \delta \equiv \varphi^2, \tag{26}$$

the NDDE (24) transforms to

$$2(\varphi\ddot{\varphi} + \dot{\varphi}^2) = [\varphi(t-T)]^3 - 2(\varphi(t))^3 + [\varphi(t+T)]^3. \tag{27}$$

The main advantage of the form (27) compared to Eqs. (24) is that it does not contain fractional powers, a feature that significantly simplifies the analysis. Finally, we normalize Eq. (27) accordingly with respect to the (yet undetermined) time delay parameter, $\tau = t/T$, $\varphi = \tilde{\varphi}/T^2$, which leads to the following normalized NDDE which will be the basis of our further analysis:

$$2(\tilde{\varphi}\tilde{\varphi}'' + \tilde{\varphi}'^2) = \tilde{\varphi}(\tau-1)^3 - 2\tilde{\varphi}(\tau)^3 + \tilde{\varphi}(\tau+1)^3. \tag{28}$$

In Eq. (28) primes denote differentiations with respect to normalized time τ. It is interesting to note that because of its noncausal nature, the NDDE (28) represents an infinite-dimensional dynamical system that cannot be solved numerically by specifying initial conditions (guesses) at a single point in τ, or even at a single interval of τ. Rather, an initial estimate over its entire wave form needs to be made before any kind of iteration or asymptotic analysis can be performed. Additional features that complicate the analysis even more are the strongly nonlinear (nonlinearizable) nature of the NDDE and the lack of a small parameter that could be used for perturbation analysis. Given these challenges we resort to an analysis based on Padé approximations.

Applying the method of Padé approximations [25], we seek the solution for the solitary wave by adopting the following simple ansatz:

$$\tilde{\varphi}(\tau) = \frac{1}{q_0 + q_2\tau^2 + q_4\tau^4 + q_6\tau^6 + q_8\tau^8 + \cdots}. \tag{29}$$

The reason for this particular choice of ansatz is twofold. First, we are interested in approximating a symmetric function in τ, so only even powers are retained in the denominator. Second, we require that the wave form decays as $\tau\to\pm\infty$ forming a single hump, which is satisfied by the structure of the selected Padé approximant (29). We note, however, that the ansatz (29) is nonunique as other forms of Padé approximants could be used in order to approximate the solitary wave (e.g., Sun *et al.* [22]). Substituting Eq. (29) into Eq. (28) and collecting like powers of τ we derive a

TABLE I. Convergence of the coefficients of the Padé approximation (24).

	q_0	q_2	q_4	q_6	q_8	(Maximum error)^2
Two-term approximation	1.14	0.17				0.2606
Three-term approximation	0.9313	0.3057	0.0392			0.0834
Four-term approximation	0.8604	0.3512	0.0696	0.0075		0.0311
Five-term approximation	0.8357	0.3669	0.0831	0.0123	0.0011	0.0128

system of nonlinear algebraic equations in terms of the coefficients q_k, with $k=1,2,\ldots$ which we truncate and solve numerically. A numerical convergence study is then performed in order to determine the limit of the truncation that guarantees convergence of the solution. For example, by retaining only four terms in the Padé approximation we derive the following system of equations for the coefficients:

$$\frac{2}{{q_0}^3} - \frac{2}{(q_0+q_2)^2} - \frac{4q_2}{{q_0}^3} = 0,$$

$$\frac{36{q_2}^2}{{q_0}^4} - \frac{16{q_2}^2}{(q_0+q_2)^2} + \frac{2}{(q_0+q_2)}\left[\frac{4{q_2}^2}{(q_0+q_2)^4} + \frac{2q_2(3q_2-q_0)}{(q_0+q_2)^4}\right] - 2q_2\left[\frac{(3q_2-q_0)}{(q_0+q_2)^5}\right] - \frac{60q_2}{{q_0}^4} = 0, \tag{30}$$

which has to be solved numerically. Moreover, at each level of approximation the resulting algebraic system for the coefficients should be solved simultaneously for all unknowns and cannot be successively parametrized by q_0. This is due to the presence of time delay in Eq. (28) which brings all the unknowns at the very first level of approximation.

In Table I we present a convergence study for the coefficients of the Padé approximation (29). It is clear that satisfactory convergence is achieved by using a five-term Padé approximation which gives an error squared of $O(10^{-2})$. In this convergence study the maximum error is estimated by computing the supremum of the difference between the Padé approximation and the exact solution at certain selected time instants. The exact solution for the solitary wave was obtained by direct numerical integration of the equations of motion (21) as discussed below. It is worthwhile mentioning that due to the applied normalizations the Padé coefficients need to be evaluated only once [by solving relations analogous to Eq. (30)], and then can be used to approximate solitary waves of arbitrary amplitudes and in systems with arbitrary parameters. Hence, the Padé coefficients listed in Table I provide a general analytical approximation of the solitary wave, which is valid for arbitrary energy levels and for general homogeneous granular chains of infinite extent.

In Fig. 8 we present the convergence of the Padé approximations (29) to the exact solitary wave for increasing number of terms. In these plots the exact solitary wave was computed by direct numerical simulations of the a homogeneous chain with $N=200$ beads subject to an impulse applied at the first bead at the free left boundary of the chain. In this system a propagating solitary wave is fully formed after the fifth bead so its wave form can be accurately estimated. From the plots in Fig. 8 we note rapid convergence of the Padé approximations to the exact solutions after five terms are included, in accordance to the results listed in Table I. Due to the applied normalizations the numerical coefficients listed in that table can be used to compute accurate analytical approximations of solitary wave in infinite granular chains with varying stiffness and mass properties and at arbitrary energy levels.

Furthermore, of significant practical importance is the relationship between the amplitude of the solitary wave and the time shift T, which is similar to relation (5) for traveling waves:

$$T = \sqrt{\tilde{\varphi}(0)}\,\delta(0)^{-1/4}. \tag{31}$$

The normalized initial condition $\delta(0)$ on the right-hand side of Eq. (31) provides a measure of the energy (amplitude) of the solitary wave. We note that from this relation we can also compute the dependence of the speed of the solitary wave on its energy (amplitude), which again is in good agreement with previously reported theoretical and numerical findings. In Fig. 9 we compare the analytical relation (31) with results obtained from direct numerical simulations, from which good agreement is observed. Recently it was demonstrated by Ahnert *et al.* [26] that solitary waves in strongly nonlinear lattices exhibit superexponential (compact) decay ($\approx \exp\{-C[3/2]^t\}$). As it may be observed from Eq. (29) the decay predicted by the Padé approximation is polynomial rather than superexponential, which means that despite a rather satisfactory accuracy of the Padé approximation of the solitary wave profile as well as of the corresponding phase shift, we still cannot state that this approximation captures the true asymptotical behavior (i.e., the superexponential decay) in the far field (far from the peak of the solitary wave). To emphasize this point, in Fig. 8(c) we depict the comparison of the five-term Padé approximation with the exact wave form derived by direct numerical simulation; it is evident that away from the peak of the wave form the difference between the two solutions increases. However, in the far field the amplitudes of the solitary wave become exponentially small, so the corresponding error by the Padé approximation becomes small.

IV. COMPARATIVE STUDY OF TRAVELING WAVES FOR FINITE N AND THE SOLITARY WAVE FOR $N\to\infty$

We now perform a comparative study of the results in an effort to provide further evidence in support of our conjecture made in Sec. II that the solitary wave in the limit $N\to\infty$ of the reduced cyclic system (1a) is the limit of the

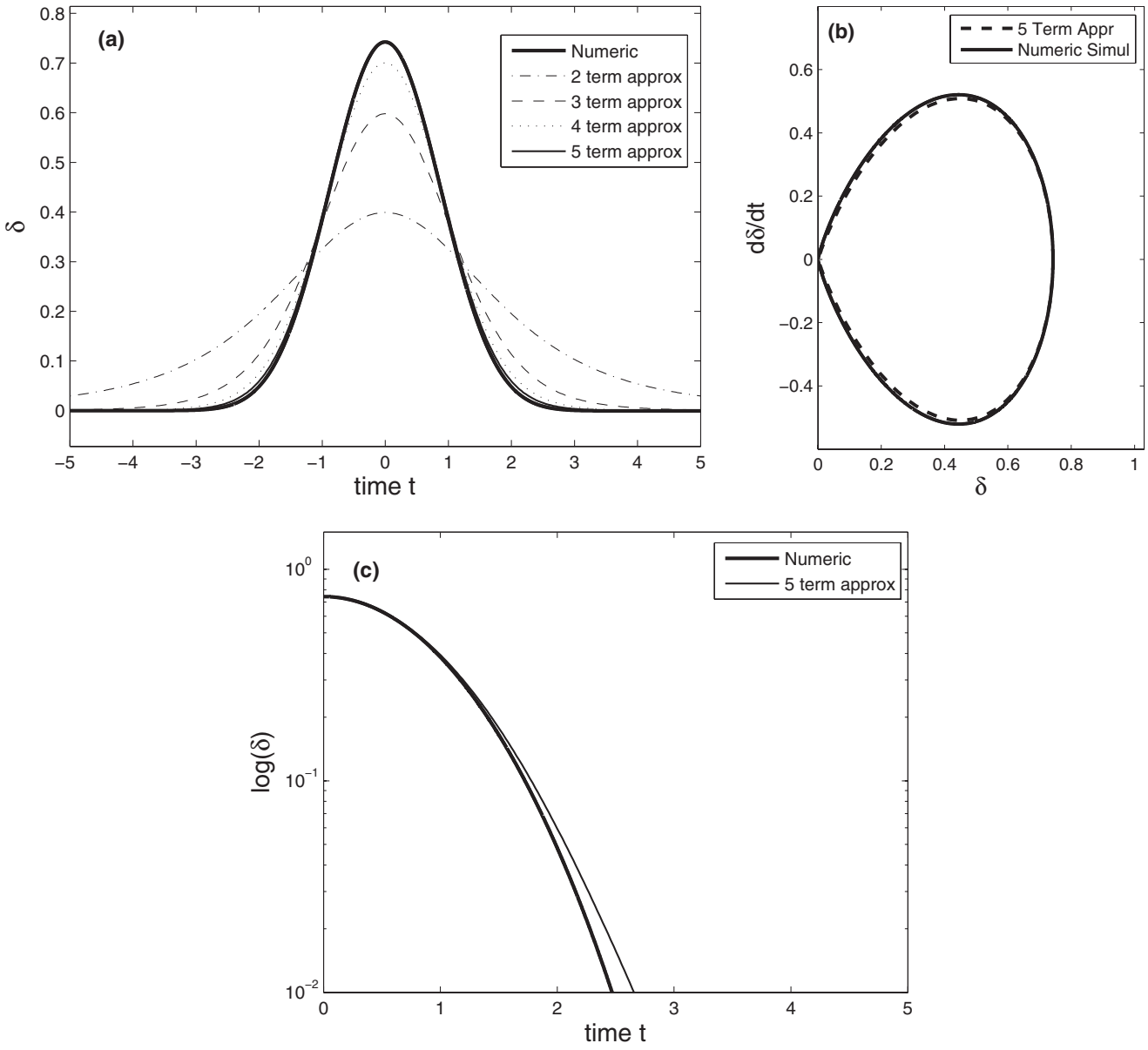

FIG. 8. Convergence of the Padé approximations to the exact solution for the solitary wave in the limit $N \to \infty$: (a) wave forms for two-, three-, four-, and five-term approximations and comparison to the exact wave form; (b) comparison between the five-term approximant and the exact solution in the phase plane $(\delta, \dot{\delta})$; and (c) comparison of the five-term approximation with the exact wave form in a logarithmic-linear plot (the base of the logarithm is 10).

countable infinity of the family of traveling waves of the systems with $N > 2$. Although this result is not formally proven in this work, there are two strong indications that this is indeed the case. First, the outlined asymptotic analysis in terms of asymmetric nonsmooth generating functions described in Sec. II indicates that for finite but large values of the cyclic periodicity index N the wave forms of the generating functions of the spatially periodic traveling waves become increasingly more asymmetric, and in the limit $N \to \infty$ degenerate to a single-hump localized solitary wave with infinite spatial periodicity. Second, by studying the amplitude (energy)-time shift plots (depicted below) it appears that the plot corresponding to the solitary wave for $N \to \infty$ provides an upper bound to the corresponding plots of the families of traveling waves with finite cyclicity index N.

Focusing on the amplitude-time shift relationships of the reduced cyclic systems with N-bead periodicity, in Fig. 10(a) we depict the theoretical plots for the out-of-phase standing wave for $N=2$ and the spatially periodic traveling waves for $N=3$ and $N=4$. These results were verified by direct numerical simulations of these solutions in a chain with 200 beads, and some of these results are also depicted in Fig. 10(a). Satisfactory correspondence of the theoretical and numerical results is noted, which confirms our findings. The corresponding velocity-time shift plots for these waves are illustrated in Fig. 10(b), where the plot for the solitary wave in the limit $N \to \infty$ is also depicted. It is worthwhile noting that comparing velocity profiles of traveling waves with that of solitary wave it is important to remember that the former possess both positive (maximum) and negative (minimum)

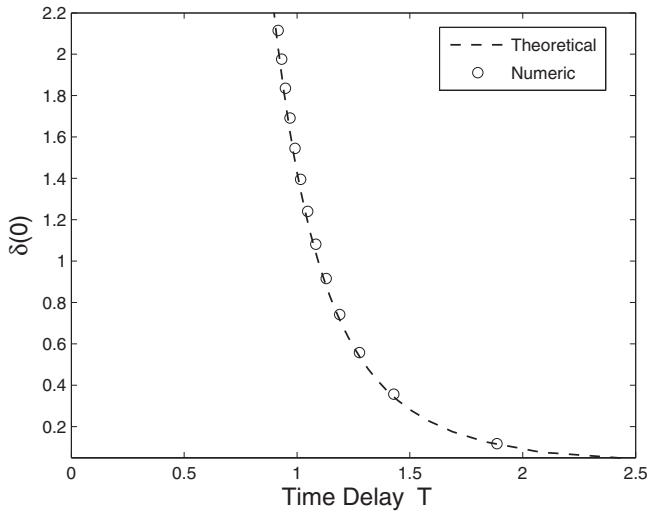

FIG. 9. Comparison between the analytical and numerical energy (amplitude)-time shift relations for the solitary wave in the limit $N\rightarrow\infty$.

velocity values due to the oscillatory nature of their motion. On the other hand, the velocity wave form of the solitary wave has only a single positive maximum value and a zero minimum value at infinity as it has a single-hump wave form. Therefore, to compare the velocity profiles of these two different types of motion we need to define relative velocities for the traveling waves, as the differences between their maximum and minimum values. These relative velocities are computed for each type of traveling-wave solution and compared to the maximum velocity of the solitary wave profile [see Figs. 10(b) and 11].

The results in Fig. 10(b) indicate that as N increases the velocity-time shift plots of the traveling waves approach the corresponding curve of the solitary wave. This provides a strong hint that the solitary wave is indeed the asymptotic limit of the countable infinity of the families of traveling waves parametrized by the cyclicity index N of the reduced system (1a). Moreover, the results depicted in Fig. 10(b) prove that the traveling waves of the reduced systems with finite N propagate with slower speeds than the solitary wave obtained in the limit $N\rightarrow\infty$, so it appears that the speed of the solitary wave studied by Nesterenko provides an upper bound to the speed for traveling-wave propagation in the homogeneous granular chain.

An additional strong hint that the solitary wave indeed represents the asymptotic limit of the families of spatially periodic traveling waves in the homogeneous granular chain is provided by the examination of the wave forms of the responses of the previously studied waves. In each plot the energies of the solutions are chosen suitably to correspond to common velocity wave amplitudes. In Fig. 11 we present a comparison of the velocity and displacement wave forms of the standing and traveling waves for $N=2$, 3, and 4 and of the solitary wave in the limit $N\rightarrow\infty$. Wave forms for the corresponding displacements are presented in Fig. 11(b). As the cyclicity index N increases the wave forms of the spatially periodic traveling waves converge to that of the solitary wave. In fact, already for $N=4$ the velocity wave form

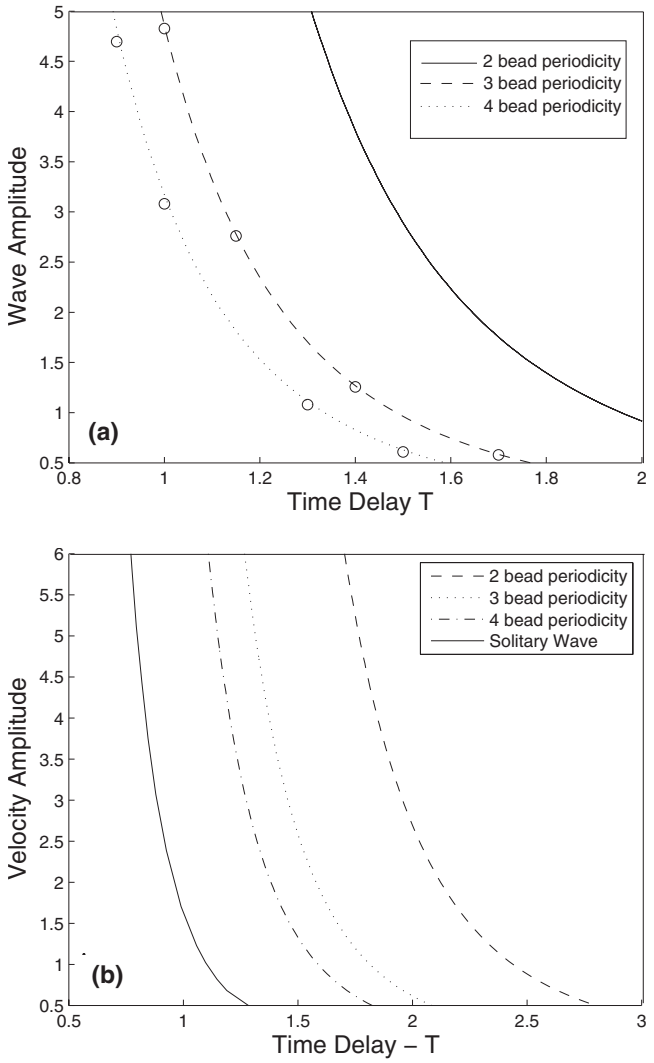

FIG. 10. Response-time shift relationships for different families of traveling waves: (a) wave amplitude-time shift plots for $N=2$ (standing waves) and $N=3,4$ (traveling waves) and (b) wave velocity-time shift plots for $N=2$ (standing waves), $N=3,4$ (traveling waves), and $N\rightarrow\infty$ (solitary wave).

of the traveling wave is nearly identical to that of the solitary wave, a result that confirms the findings of previous works (e.g., Nesterenko *et al.* [1,23]) that the solitary wave has a finite spatial extent as it propagates through the granular chain.

Finally, in Fig. 12 we depict the time series for the velocity wave forms of the standing wave for cyclic periodicity $N=2$ and of the traveling waves for $N=3$ and 4. All waves possess identical maximum velocities. In each case, the regions of free flight (i.e., of bead separation) correspond to constant velocities. We note that for cyclic periodicity $N=2$ there is no bead separation and no traveling-wave propagation is possible. For $N=3$ and 4 the regions of free flight progressively increase with increasing N, rendering the wave form of the traveling wave increasingly more asymmetric. In the limit $N\rightarrow\infty$ the region of free flight tends to infinity, the spatial period of the wave tends to infinity, and the traveling wave degenerates to the propagating solitary wave studied by Nesterenko.

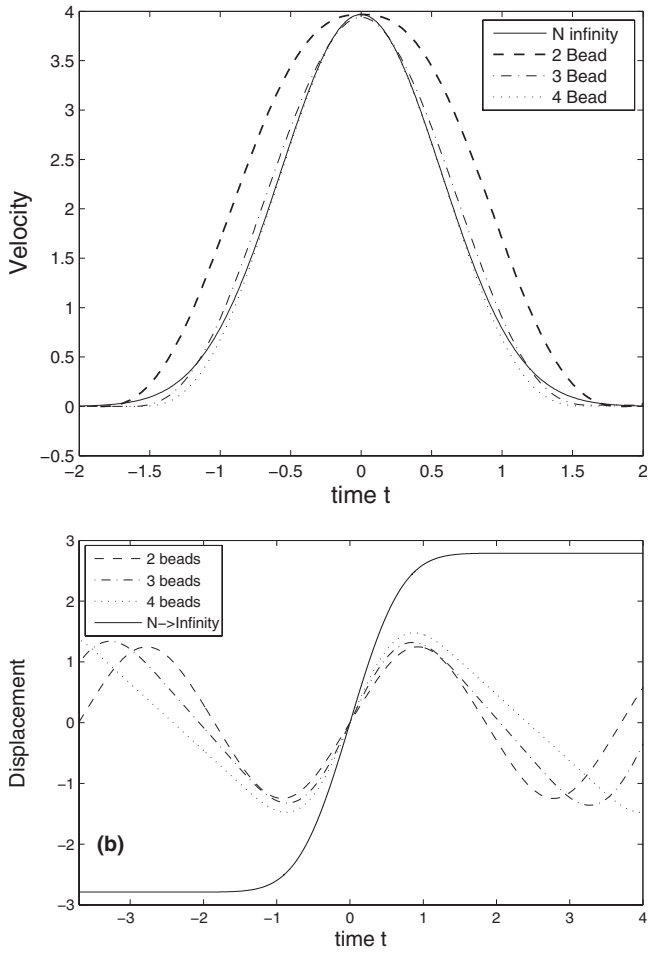

FIG. 11. Comparison of response wave forms of waves for systems with finite cyclic periodicity index N and the solitary wave as $N \to \infty$: (a) velocity wave forms and (b) corresponding displacement wave forms.

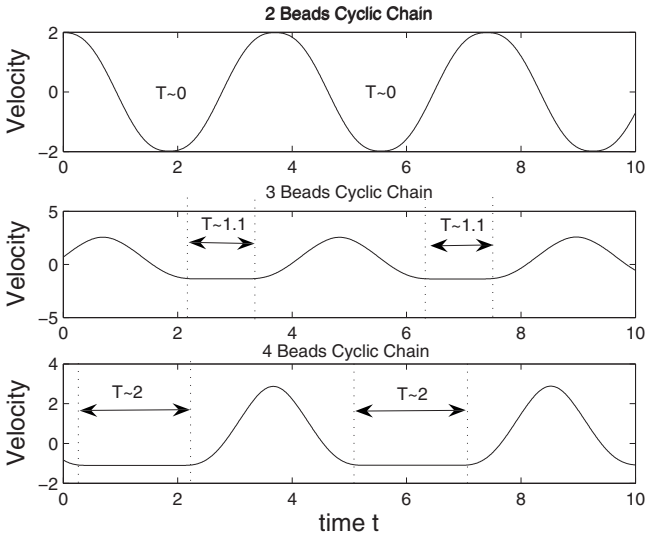

FIG. 12. Velocity wave forms for waves with cyclic periodicities $N=2$, 3, and 4.

V. CONCLUDING REMARKS

We proved the existence of a class of strongly nonlinear traveling waves in one-dimensional homogeneous granular chains with no precompression. Until now the only traveling-wave solutions known in this class of systems were the single-hump solitary waves computed by Nesterenko in the continuum approximation limit. The nonsmooth nature of the traveling waves considered herein prevented the use of a continuum approach; instead, we analyzed directly the discrete equations of motion by imposing periodic boundary conditions or, equivalently, cyclic symmetry. This enabled us to systematically study the different families of traveling waves parametrized by the index of cyclicity N, and to fully account for nonsmooth effects caused by bead separation. The speed of propagation of the traveling waves is lower than the corresponding speed of the solitary wave studied by Nesterenko and strongly depends on energy as they are strongly nonlinear. The asymmetry of their wave forms is a direct consequence of the asymmetric law of Hertzian interaction between beads and becomes progressively stronger as the index of cyclic periodicity increases. It is interesting to note, however, that in the limit of infinite index N the asymmetry in the wave form is eliminated as the families of traveling waves converge to the single-hump solitary wave studied by Nesterenko.

In addition, we proved the existence of an additional class of stable strongly localized out-of-phase standing waves in homogeneous granular chains even in the absence of precompression or disorder. Until now such localized solutions were known to exist only in granular chains with strong precompression. Similarly to the families of traveling waves, these standing waves are also highly asymmetric and to analyze them one should consider directly the discrete governing equations of motion instead of applying continuum approximations.

In summary, our findings indicate that homogeneous granular chains with no precompression possess complex intrinsic nonlinear dynamics, including intrinsic nonlinear energy transfer and localization phenomena. The families of traveling waves studied herein provide an additional strongly nonlinear mechanism for transferring energy through homogeneous granular chains, in addition to the solitary wave studied by Nesterenko. In contrast, the excitation of localized standing waves such as the ones reported in this work leads to motion confinement and prevents energy transfer in granular chains. Current work by the authors and their co-workers aims to study the robustness of the reported traveling and standing waves to precompression and disorder.

ACKNOWLEDGMENTS

The authors would like to thank Professor Valery Pilipchuk for helpful suggestions, comments, and discussions. This work was funded by U.S. ARO MURI Grant No. W911NF-09-1-0436. Dr. David Stepp is the grant monitor.

[1] V. Nesterenko, *Dynamics of Heterogeneous Materials* (Springer, New York, 2001).
[2] V. F. Nesterenko, J. Appl. Mech. Tech. Phys. **24**, 733 (1983).
[3] A. Chatterjee, Phys. Rev. E **59**, 5912 (1999).
[4] A. N. Lazaridi and V. F. Nesterenko, J. Appl. Mech. Tech. Phys. **26**, 405 (1985).
[5] C. Coste *et al.*, Phys. Rev. E **56**, 6104 (1997).
[6] R. S. MacKay, Phys. Lett. A **251**, 191 (1999).
[7] J. Y. Ji and J. Hong, Phys. Lett. A **260**, 60 (1999).
[8] G. Friesecke and J. A. D. Wattis, Commun. Math. Phys. **161**, 391 (1994).
[9] R. H. Rand, J. Appl. Mech. **38**, 561 (1971).
[10] L. A. Month and R. H. Rand, J. Appl. Mech. **44**, 782 (1977).
[11] L. A. Month and R. H. Rand, J. Appl. Mech. **47**, 645 (1980).
[12] L. A. Month, Ph.D. thesis, Cornell University, 1979.
[13] A. F. Vakakis *et al.*, *Normal Modes and Localization in Nonlinear Systems* (John Wiley and Sons, New York, 1996).
[14] S. Wiggins, *Introduction to Nonlinear Dynamics and Chaos* (Springer Verlag, New York, 1990).
[15] G. Theocharis *et al.*, e-print arXiv:0906.4094.
[16] N. Boechler and C. Daraio, Proceedings of the ASME IDETC/CIE 2009, San Diego, CA, 2009 (unpublished), Paper No. DETC2009-87427.
[17] V. N. Pilipchuk, J. Appl. Mat. Mech. **49**, 572 (1985).
[18] V. N. Pilipchuk, Dokl. Akad Nauk. UkrSSR Ser. A **4**, 37 (1988).
[19] V. N. Pilipchuk, J. Sound Vib. **192**, 43 (1996).
[20] V. N. Pilipchuk and G. A. Starushenko, J. Appl. Math. Mech. **61**, 265 (1997).
[21] G. A. Starushenko *et al.*, Int. J. Heat Mass Transfer **45**, 3055 (2002).
[22] S. Sen *et al.*, Phys. Rep. **462**, 21 (2008).
[23] V. F. Nesterenko *et al.*, Phys. Rev. Lett. **95**, 158702 (2005).
[24] C. Daraio *et al.*, Phys. Rev. E **73**, 026610 (2006).
[25] E. Emaci *et al.*, Nonlinear Dyn. **13**, 327 (1997).
[26] K. Ahnert *et al.*, Phys. Rev. E **79**, 026209 (2009).